

Design of a Novel THz Sensor for Structural Health Monitoring Applications

J. P. Pavia^{1,2,*}, M. A. Ribeiro^{1,2}, C. K. Sarikaya³, D. Akbar³, H. Altan³, and N. Souto^{1,2}

¹University Institute of Lisbon - ISCTE-IUL, Av. das Forças Armadas, 1649-026 Lisbon, Portugal

²Instituto de Telecomunicações, Av. Rovisco Pais, 1049-001 Lisbon, Portugal

³Department of Physics, Middle East Technical University, 06800, Ankara, Turkey

*Joao_Pedro_Pavia@iscte-iul.pt

Abstract—In this paper, we propose a study on the characterization, design and simulation of a THz sensor for applications in Structural Health Monitoring (SHM). The proposed sensor is assembled using two frequency selective surfaces (FSSs) based on metamaterial wire resonators. We present a theoretical model to describe its electromagnetics which is used not only to understand the physical principles underlying the functioning of the sensor but also to determine a set of optimized parameters for its operation in the THz window from 395 GHz to 455 GHz. We present our numerical simulations, involving both electromagnetic and mechanical simulation techniques, to determine the reflectance profile of the sensor as a function of applied force. In this study we considered the possibility of using two thermoplastic polymers as host materials: High-Density PolyEthylene (HDPE) and PolyTetraFluoroEthylene (PTFE). The two sensors have a good dynamic range and comparable characteristics. However, we found that with HDPE it is possible to construct a sensor with a more linear response, although not as sensitive as in the case of PTFE. With HDPE we are able to pass from a situation of full transparency to almost full opacity using only its linear operating zone.

Index Terms—Filter, Frequency Selective Surfaces (FSSs), Sensors, Structural Health Monitoring (SHM), Terahertz (THz).

I. INTRODUCTION

Structural Health Monitoring (SHM) plays a major role in industry and engineering. It is a multidisciplinary field that is dedicated to the implementation of new methodologies that allow the monitoring of the state of conservation of buildings, and other engineering structures. With the emergence of new technologies related to THz imaging, some interesting developments have been proposed in the past few years which relate SHM to the THz range. For example, the utilization of frequency selective surfaces (FSSs) allows for the construction of compact devices, similar to Microelectromechanical systems (MEMS), which can be easily integrated onto the surface of the structures. Since these structures are so small, given the high values of frequency in the THz range, it is possible to perform structure monitoring without harming functionality and aesthetics [1], [2]. In particular, FSSs are metamaterials especially design to offer higher frequency selectivity and resolution when compared with naturally available materials. They can deliver strong enhancement and localization of fields, being especially suited for the development of wireless strain sensors that can operate at the microwave and terahertz ranges

[3]. It is therefore foreseeable that these structures have a great potential for application in all areas related to metamaterials but also in areas related to SHM.

Despite the wide range of available methodologies and sensors, there is a lack of highly selective sensors for the terahertz domain. The application of THz technologies to SHM is a new field of research with few articles published on the topic [2-6]. In addition to the papers addressing THz sensors, there is also a significant amount of literature adopting THz imaging as the primary method for detecting structural damage [4]. An interesting technology is described in [5], where the authors propose a terahertz sensor to measure vibrations behind optically opaque barriers. As a result, the displacement caused by a change in mechanical loading can be measured using this sensor and surface irregularities can be found.

The development of THz stress sensors based on metal mesh filters is described by C. Duque et al. and W. J. Otter *et al.* in [2, 6]. In this sensors, their resonances is due to the periodicity of the unit cells in the direction of propagation and, according to the authors, these sensors can be used in several applications, including SHM. Their integration into the structures allow to detect cracks and other kind of damages, since, in this type of critical situations, it is known that the transmittance values of the sensors decrease abruptly.

This paper aims to provide a comprehensive study on the characterization, design and simulation of two stress sensors for the THz domain using HDPE and PTFE host materials. We seek for solutions that maximize the sensitivity of the design and with that in mind we developed a theoretical model using network theory for the optimization of the sensor parameters prior to simulation.

The paper is organized as follows: In section II we present an overview of the operation principle of the sensor. Based on network theory [7], a theoretical model is outlined for the device and the most relevant parameters to the design are identified. Numerical simulation that corroborate the working principle of the sensors are presented in section III. Here we focus on two possibilities regarding the construction of the sensor. One using HDPE and another using PTFE. The results obtained, involve both electromagnetic and mechanical simulations, and allow to determine the characteristic curves of the sensors for reflectance as a function of applied force. Finally, the conclusions are outlined in section IV.

II. CIRCUIT THEORY AND DESIGN

A. Operation principle and basic circuit structure

In Fig. 1a we show the geometry of the proposed sensor. It consists of a dielectric host material of length l and two arrays of wires separated by a distance $l/3$. The distance between wires is d and their radius is a . Later, we will see that an appropriate choice of the ratio d/a enhances the resonant effects of the structure and thereby greater sensitivity is obtained. For now, we explain the principle of operation of the device.

The sensor is designed so that when it is not compressed its frequency response has the form shown in figure 1b (see red curve). When compressed (in the direction of the green arrows shown in Fig. 1a) its frequency response will change because the distance between wires is reduced. The green and blue curves in Fig. 1b illustrate the expected behavior in the frequency response. The blue curve corresponds to maximum compression and the green curve to half compression.

The sensor operates at the target frequency (see Fig. 1b). Without compression the sensor is completely transparent at this frequency, allowing all the radiation to pass through. This condition is indicated by a red circle in Fig. 1b. In contrast, when the sensor is fully compressed it becomes opaque, and incident radiation is completely reflected. This situation is also identified in Fig. 1b (blue circle). In between, all levels of reflectance exist and the sensor is designed so that its response is approximately linear in this region of operation.

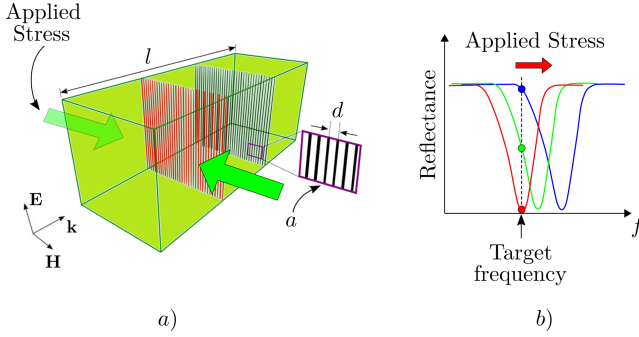


Fig. 1. a) THz sensor geometry and b) operation principle.

In order to analyze the structure we have developed the simplified two-port network model shown in Fig. 2. In this model, Z_p is the impedance of the port, Z is the characteristic impedance of the dielectric slab material, β is the propagation constant, l is the length of the structure and Y the admittance of the embedded grids.

The admittance Y can be expressed as

$$Y = j \frac{\lambda}{d} \frac{2Z^{-1}}{\ln \left(2 \left[1 - \cos \left(\frac{2\pi a}{d} \right) \right] \right)} \quad (1)$$

where λ is the wavelength.

From the model, we first obtained the transmission matrix of the structure. Then, using the formulas for the conversion between two-port network parameters given in [7] we derived the scattering parameters:

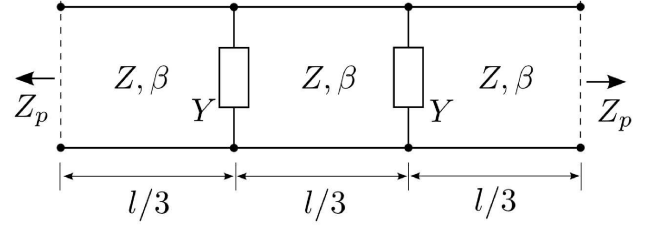


Fig. 2. Equivalent microwave network circuit of the THz filter.

$$S_{11} = S_{22} = \frac{2 z_1 z_3 z + z_1^2 z - z^{-1}}{2 (z_1 + z_3) 2 z_1 z_3 z + z_1^2 z + z^{-1}} \quad (2)$$

$$S_{12} = S_{21} = \frac{2 z_3}{2 (z_1 + z_3) 2 z_1 z_3 z + z_1^2 z + z^{-1}} \quad (3)$$

where $z = Z/Z_0$ is the normalized impedance of the slab. Z_0 is the impedance of free space and since we assume the structure is immersed in free-space we have $Z_p = Z_0$.

The impedances z_1 , z_2 and z_3 are also normalized impedances which are given by

$$z_1 = z_2 = A/B, \quad z_3 = B^{-1} \quad (4)$$

with coefficients A and B defined as

$$A = (4 + Z^2 Y^2) \cos^3(\beta l) - (3 + Z^2 Y^2) \cos(\beta l) + 3iZY \sin(\beta l) - 4iZY \sin^3(\beta l) - 1 \quad (5)$$

$$B = ZY \cos^3(\beta l) - 2ZY \cos(\beta l) + i(3 + Z^2 Y^2) \sin(\beta l) - i(4 + Z^2 Y^2) \sin^3(\beta l) \quad (6)$$

The wires are tuned so that in addition to the reflected and transmitted waves only evanescent modes exist in the vicinity of the structure, allowing us to control the energy that is transmitted and reflected. A diagram illustrating the allowed modes of the structure is shown in Fig. 3. Here we are assuming that the wires are oriented along y and spaced apart along z . As can be seen, we can control the position of the modes in the diagram by adjusting the wire radius. Then we can adjust the distance between wires to control the bandwidth of the frequency response. The smaller the bandwidth the more sensitive the sensor is. From the theoretical model it was possible to verify that the bandwidth decreases as Y increases. Moreover, according to Eq. 1, Y is increased as we approach the limit $a/d = 1/6$ where it grows to ∞ . In practice, however, this value cannot be achieved because of the resistance of the wires and because in that limit the formula is only an approximation (formula is only valid for $d \ll \lambda$ and $a \ll d$). However, we use this formula as a starting point for our simulations to determine the best relation a/d that is also physically attainable.

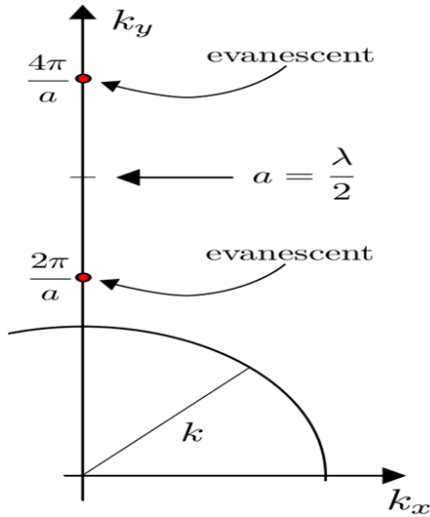


Fig. 3. Diagram of the dispersion relation.

III. NUMERICAL RESULTS

A. Choice of parameters

We used the theory described above to determine a starting point for the sensor parameters assuming a frequency window in the THz range between 395 and 455 GHz. We have considered two kinds of host materials in our analysis: PTFE with a relative dielectric constant $\epsilon_r = 2.1$ and HDPE with $\epsilon_r = 2.4$. Then we performed several electromagnetic and mechanical simulations to fine tune the parameters and we found a set that fits our requirements:

- structure length, $l = 1.42$ mm;
- radius of the wires, $a = 0.0002$ mm;
- distance between wires $d \in [0.015, 0.02]$;

In the simulations, the distance between wires is expressed as a range in order to account for the possibility of having various levels of compression. Taking into account the mechanical characteristics of the host materials, we have considered that it is possible to compress the sensor up to 25 % of its original size without destroying or deforming it definitively. According to our preliminary theoretical study this limit is sufficient to ensure that the filter works correctly in the desired frequency range. In fact, HDPE is a thermoplastic which is known for its high resistivity regarding stress cracking. It can handle temperatures from 173.15 to 353.15 Kelvin (K) and is widely used in industry because it is a cheap and easy to mold material. PTFE has also some special features, such as the capability of maintaining high strength and good flexibility at temperatures above 194K. Furthermore, according to Naftaly and Dudley, silicon and plastics such as HDPE and PTFE are key terahertz materials since they are relatively easy to compress and exhibit low losses and low dispersion in the frequency band from 0.1 to 5 THz, [8].

B. Electromagnetic analysis with HDPE host

Fig. 4 shows the numerical simulation, using Finite Element Method, for the reflectance of the sensor as a function of fre-

quency for various degrees of compression. In the simulations, we considered only a unit cell consisting of a single wire. We impose the necessary boundary conditions to artificially create the solution of an array of wires separated a distance d apart and extending infinitely in the direction of the wires. This is clearly an approximation of the real problem, but this was what we understood as reasonable in order to accomplish the work without implementing a finite elements solution that would require a more in-depth study of the method. In particular, we did not consider the losses of PTFE and HDPE because these materials have very low losses in the THz range and this brought significant simplification to our implementation. HDPE has a loss tangent $\tan(\delta) = 1.0 \times 10^{-4}$ and PTFE has $\tan(\delta) = 0.0002$ which makes them transparent to THz radiation (this was one of the reasons they were chosen for this work).

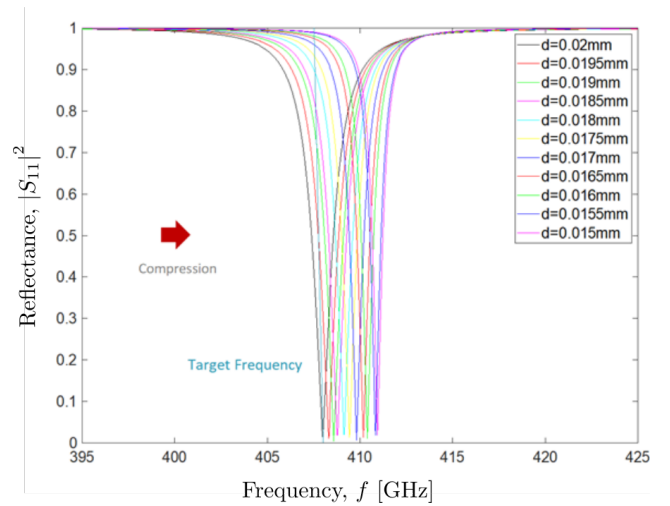


Fig. 4. Reflectance in the frequency domain as a function of applied compression for HDPE host.

Compression is modeled by reducing the distance between wires and we have considered a step size of $0.5 \mu\text{m}$ starting from the value 0.02 mm (uncompressed state) until the sensor is compressed to 25 % of its original size (0.015 mm). As can be seen, as the sensor is compressed its resonance frequency is shifted to higher frequencies. Without compression the sensor resonance is at 408 GHz and when fully compressed at 411 GHz. Between these two extreme states there was a total shift in the frequency of 3 GHz. There is a vertical line in the figure identifying the target frequency (408 GHz) and it can be clearly seen that the sensor has an excellent dynamic range along this curve. That is, as the sensor is compressed it goes from full transparency to full opacity.

When the distance between wires is reduced of $0.5 \mu\text{m}$, the average increase of the resonant frequency is 300 MHz. As the sensor is compressed, the bandwidth at 3 dB is reduced from 2.1 GHz (without compression) to 1 GHz (fully compressed), which represents a decrease of more than 50 %. Some distortion in the sensor response is expected for this reason.

C. Electromagnetic analysis with PTFE host

The electromagnetic simulations for the PTFE case are shown in Fig. 5. The behavior is the same as that observed for HDPE but the resonances now occur at higher frequencies because the materials have different constitutive parameters. Without compression, the sensor resonates at 437.5 GHz and with full compression at 440.7 GHz. This corresponds to a total shift in the value of the resonant frequency of 3.2 GHz. Once again, the sensor has a very good dynamic range at the target frequency (437.5 GHz) where the reflectance is very near to zero without compression and near to one at full compression. We thus see that the sensor has comparable characteristics to the case with HDPE regardless of the fact they are using different host materials. The bandwidth at 3

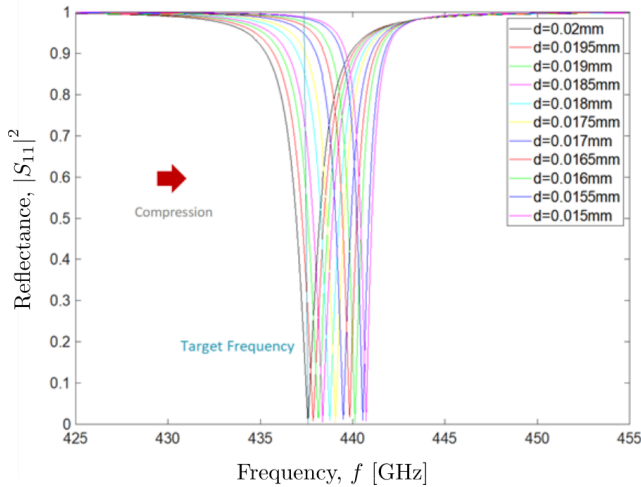


Fig. 5. Reflectance in the frequency domain as a function of applied compression for PTFE host.

dB is 2.2 GHz at the target frequency (without compression) and 1.1 GHz at full compression, which represents a decrease of 50 % in the bandwidth. We have already explained that this aspect introduces some distortion in the sensor response but this distortion is very small and can be interpreted as a saturation which is noticeable when the sensor is compressed. Also worth mentioning is that the progression of the resonance frequency as the sensor is compressed is approximately linear. In this case, there is an average increase of 320 MHz in the resonance frequency whenever the sensor is compressed 0.5 μm . This result is similar to what we had obtained for PTFE.

D. Mechanical Analysis

Mechanical simulations were also performed to obtain the reflectance as a function of the applied force on the sensor. For these simulations we used an open source software called Elmer that uses the finite element method to determine the mechanical deformation of a structure from the applied force or pressure. We assume the force is applied uniformly along the entire lateral surfaces of the sensor. In the case of the electromagnetic simulations we considered what we call the unit cell of the structure and artificially created boundary

conditions to reflect the symmetry of the wires. It was implied in this study that there are enough wires for the incident radiation to see a homogeneous structure. In the case of the mechanical simulations we took into account that the number of wires in the array influences the strain-stress curves. For this reason, several scenarios with 10, 30, 50 and 70 wires were considered. Fig. 6 shows the reflectance of the sensor as

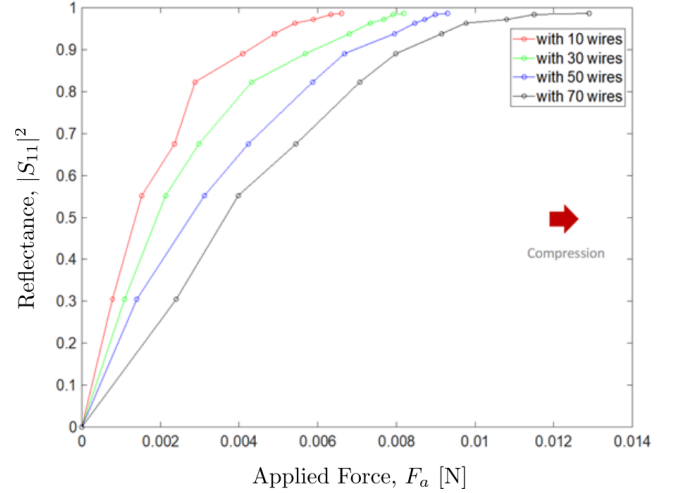


Fig. 6. Reflectance as a function of applied force 10, 30, 50 and 70 wires and a sensor assembled with HDPE.

a function of applied force for a HDPE host. These curves were obtained as follows: first, we performed mechanical simulations to determine the compression of the sensor as a function of the applied force. Then we use this information and Fig. 4 To obtain the reflectance of the sensor as a function of force.

A first aspect worth mentioning is that the number of wires has a great influence on the linearity of the response. The higher the number of wires the more linear the sensor response is. Due to limitations of computational power, it was only possible to make simulations with a maximum of 70 wires but the results suggest that by increasing the number of wires the sensor response would approach the linear case. All the curves present saturation for high values of applied force. For 70 wires, in particular, when the applied force is greater than 8 mN the sensor saturates. This behavior is justified by the mechanical characteristics of the materials we used to build the sensor but will certainly have a small contribution from the narrowing of the electromagnetic bandwidth referred above. Note however that for 8 mN the sensor reflects almost all the incident wave (aprox. 90 %) and we conclude that it has an approximately linear response in the dynamic range of interest.

The results for PTFE host are shown in Fig. 7. As can be seen, the curves obtained for this sensor model are not as linear as before. However, the sensor built with this material is more sensitive since one can cover the entire dynamic range with much less applied force. There is however a linear operating zone if it is acceptable to work with reflectances between 0.2 and 0.8.

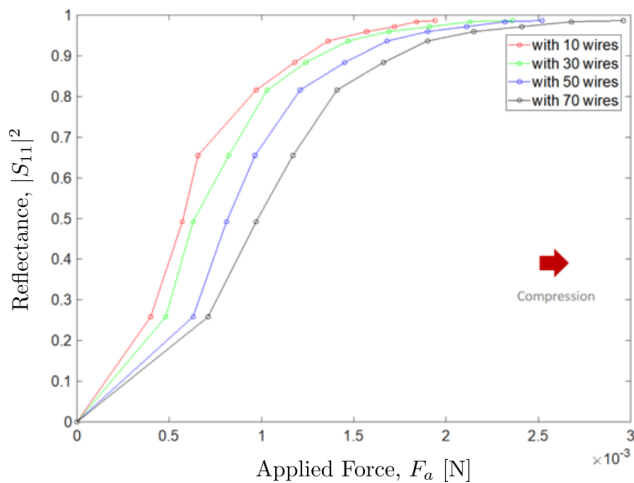


Fig. 7. Reflectance as a function of applied force 10, 30, 50 and 70 wires and a sensor assembled with PTFE.

IV. CONCLUSIONS

In this paper we proposed a theoretical model and presented results of our simulations to demonstrate the working principle of a new stress sensor for the THz domain. The architecture is based on two FSSs and we discussed the methodology to find a good selection of geometric parameters to fine tune the FSSs, which is directly related to the sensitivity of the sensor. Numerical simulations were carried out to determine the reflectance as a function of applied force assuming the possibility of constructing the sensor with two different plastic host materials: HDPE and PTFE. Both solutions converged on interesting results. For example, with HDPE host it is possible to obtain a sensor whose response is quite linear and with a very good dynamic range. With PTFE the solution is not so linear and does not have such a good dynamic range, but it is much more sensitive. The differences are due to mechanical factors that characterize the two materials but also because they have different electromagnetic properties.

The proposed design can be easily adapted to several interesting applications related to SHM. Although we are not applying our design to a specific application here, with the present study we found a methodology that allows us to draw the best combination of materials and geometric parameters based on the requirements of the application for which the sensor is being designed.

ACKNOWLEDGMENT

The authors acknowledge financial support by Fundação para a Ciência e a Tecnologia under the project TUBITAK/0002/2014.

REFERENCES

- [1] S. Lucyszyn, (Ed.). *Advanced RF MEMS (The Cambridge RF and Microwave Engineering Series)*. Cambridge, Cambridge University Press, 2010.
- [2] C. Duque and M. A. Ribeiro, "Effect of uniaxial compression in the transmittance of a novel terahertz sensor for structural health monitoring," *Proceedings of Loughborough Antennas and Propagation Conference 2013*, pp. 122126, 2013.

- [3] B. Ozbey, E. Unal, H. Ertugrul, O. Kurc, C. Puttlitz, V. Erturk, A. Altintas and H. Demir, "Wireless Displacement Sensing Enabled by Metamaterial Probes for Remote Structural Health Monitoring," *Sensors*, vol. 14, no. 1, pp. 1691-1704, 2014.
- [4] S. Fan, T. Li, J. Zhou, X. Liu, X. Liu, H. Qi and Z. Mu, "Terahertz non-destructive imaging of cracks and cracking in structures of cement-based materials," *AIP Advances*, vol. 7, no. 11, p. 115202, 2017.
- [5] J. Chen and S. Kaushik, "Terahertz Interferometer That Senses Vibrations Behind Barriers," *IEEE Photonics Technology Letters*, vol. 19, no. 7, pp. 486-488, 2007.
- [6] W. J. Otter, F. Hu, S. Hanham, A. S. Holmes, W. T. Pike, N. Klein, M. A. Riberio and S. Lucyszyn, "Terahertz Metamaterial Devices," *Proceedings of The International Conference on Semiconductor Mid-IR and THZ Materials and Optics SMMO 2016*, pp.25, 2016.
- [7] D. M. Pozar, *Microwave Engineering*, 2nd ed., Wiley, 1998, pp.182-250.
- [8] M. Naftaly and R. Dudley, "Introduction to Terahertz - The ins and outs of terahertz technologies, what it does and how it works," NPL - National Physics Laboratory, 2017.